

AFRL-ML-WP-TP-2007-457

**EFFECT OF AI ADDITION ON GLASS
FORMING STABILITY OF Ca-Mg-Zn-
Cu BASED BULK METALLIC
GLASSES (PREPRINT)**



O.N. Senkov, J.M. Scott, and Daniel B. Miracle

APRIL 2007

Approved for public release; distribution unlimited.

STINFO COPY

**The U.S. Government is joint author of this work and has the right to use, modify,
reproduce, release, perform, display, or disclose the work.**

**MATERIALS AND MANUFACTURING DIRECTORATE
AIR FORCE RESEARCH LABORATORY
AIR FORCE MATERIEL COMMAND
WRIGHT-PATTERSON AIR FORCE BASE, OH 45433-7750**

REPORT DOCUMENTATION PAGE

*Form Approved
OMB No. 0704-0188*

The public reporting burden for this collection of information is estimated to average 1 hour per response, including the time for reviewing instructions, searching existing data sources, gathering and maintaining the data needed, and completing and reviewing the collection of information. Send comments regarding this burden estimate or any other aspect of this collection of information, including suggestions for reducing this burden, to Department of Defense, Washington Headquarters Services, Directorate for Information Operations and Reports (0704-0188), 1215 Jefferson Davis Highway, Suite 1204, Arlington, VA 22202-4302. Respondents should be aware that notwithstanding any other provision of law, no person shall be subject to any penalty for failing to comply with a collection of information if it does not display a currently valid OMB control number. **PLEASE DO NOT RETURN YOUR FORM TO THE ABOVE ADDRESS.**

1. REPORT DATE (DD-MM-YY) April 2007			2. REPORT TYPE Journal Article Preprint		3. DATES COVERED (From - To)	
4. TITLE AND SUBTITLE EFFECT OF Al ADDITION OF GLASS FORMING STABILITY OF Ca-Mg-Zn-Cu BASED BULK METALLIC GLASSES (PREPRINT)			5a. CONTRACT NUMBER FA8650-04-D-5233			
			5b. GRANT NUMBER			
			5c. PROGRAM ELEMENT NUMBER 62102F			
6. AUTHOR(S) O.N. Senkov and J.M. Scott (UES, Inc.) Daniel B. Miracle (AFRL/MLLMD)			5d. PROJECT NUMBER 2311			
			5e. TASK NUMBER 00			
			5f. WORK UNIT NUMBER 02			
7. PERFORMING ORGANIZATION NAME(S) AND ADDRESS(ES) UES, Inc. 4401 Dayton-Xenia Road Dayton, OH 45432-1894			Metals Branch/Metals Development Team (AFRL/MLLMD) Metals, Ceramics & Nondestructive Evaluation Division Materials and Manufacturing Directorate Air Force Research Laboratory, Air Force Materiel Command Wright-Patterson Air Force Base, OH 45433-7750		8. PERFORMING ORGANIZATION REPORT NUMBER	
9. SPONSORING/MONITORING AGENCY NAME(S) AND ADDRESS(ES) Materials and Manufacturing Directorate Air Force Research Laboratory Air Force Materiel Command Wright-Patterson AFB, OH 45433-7750			10. SPONSORING/MONITORING AGENCY ACRONYM(S) AFRL-ML-WP			
			11. SPONSORING/MONITORING AGENCY REPORT NUMBER(S) AFRL-ML-WP-TP-2007-457			
12. DISTRIBUTION/AVAILABILITY STATEMENT Approved for public release; distribution unlimited.						
13. SUPPLEMENTARY NOTES Journal article submitted to Metallurgical and Materials Transactions A. This paper contains color content. The U.S. Government is joint author of this work and has the right to use, modify, reproduce, release, perform, display, or disclose the work. PAO Case Number: AFRL/WS 07-1030, 25 Apr 2007.						
14. ABSTRACT The effect of Al addition on glass forming ability and glass stability of Ca-Mg-Zn, Ca-Mg-Cu, and Ca-Mg-Zn-Cu alloys was studied. The glassy alloys were produced by a copper mold casting method as wedge-shaped samples with thicknesses varying from 0.5 mm to 10 mm. Thermal properties, such as the glass transition, crystallization and melting temperatures, as well as heats of crystallization and melting, were determined for the produced glasses. Partial substitution of Zn and/or Cu with Al was found to generally reduce the glass forming ability; however, it improves the glass stability.						
15. SUBJECT TERMS Aluminum, glass forming, glass stability, bulk metallic glasses						
16. SECURITY CLASSIFICATION OF:		17. LIMITATION OF ABSTRACT: SAR		18. NUMBER OF PAGES 26	19a. NAME OF RESPONSIBLE PERSON (Monitor) Daniel B. Miracle	
a. REPORT Unclassified	b. ABSTRACT Unclassified	c. THIS PAGE Unclassified			19b. TELEPHONE NUMBER (Include Area Code) N/A	

Effect of Al addition on glass forming ability and glass stability of Ca-Mg-Zn-Cu based bulk metallic glasses

O.N. Senkov^{1*}, J.M. Scott¹ and D.B. Miracle

Air Force Research Laboratory, Materials and Manufacturing Directorate, Wright-Patterson AFB, OH 45433, USA

¹ UES, Inc., 4401 Dayton-Xenia Rd, Dayton, OH 45433, USA

Abstract

The effect of Al addition on glass forming ability and glass stability of Ca-Mg-Zn, Ca-Mg-Cu, and Ca-Mg-Zn-Cu alloys was studied. The glassy alloys were produced by a copper mold casting method as wedge-shaped samples with thicknesses varying from 0.5 mm to 10 mm. Thermal properties, such as the glass transition, crystallization and melting temperatures, as well as heats of crystallization and melting, were determined for the produced glasses. Partial substitution of Zn and/or Cu with Al was found to generally reduce the glass forming ability; however, it improves the glass stability.

1. Introduction

Low density bulk metallic glasses (BMGs) in Ca-Mg-Zn, Ca-Mg-Cu and Ca-Mg-Zn-Cu systems have recently been developed [1-10]. These metallic glasses represent a new group (7th group by Takeuchi and Inoue [11]) of BMGs. They are based on two simple metals (Ca and Mg), while all other BMGs rely on transition metals. The Ca- based glasses have low density (~2000 kg/m³) and their Young's modulus values (~20-35 GPa) are comparable to the modulus of human bones [12]. Many of these BMGs have very good glass forming ability (GFA) and fully amorphous plates and rods with thickness or diameter larger than 10 mm can be easily produced by casting [8-10]. Although Ca-Mg-Zn-Cu glasses have a wide temperature range of super-cooled liquid ($\Delta T_x = T_x - T_g \sim 30-70$ °C), they have low glass transition temperature ($T_g \sim 100-150$ °C) and crystallization temperature ($T_x \sim 130-180$ °C), i.e. low glass stability (GS) against crystallization

* Corresponding author. E-mail: oleg.senkov@wpafb.af.mil.

at near ambient temperatures. The ternary Ca-Mg-Zn and Ca-Mg-Cu glassy alloys also have marginal oxidation and corrosion resistance [13-15]. Quaternary Ca-Mg-Zn-Cu BMGs have better oxidation and corrosion resistance, which improves even further with addition of Al [15]. Partial substitution of Cu and/or Zn with Al also reduces the density of these alloys. Estimations show that every 1 at.% Al added in place of Zn will reduce the density in Ca-Mg-Zn alloys by ~ 1%. Unfortunately, there is no data available on the effect of Al addition on GFA and GS of Ca-Mg-Zn-Cu metallic glasses.

In the present work we produced several new Ca-Mg-Al-Zn, Ca-Mg-Al-Cu and Ca-Mg-Al-Zn-Cu bulk metallic glasses by partial substitution of Zn and/or Cu with Al in the baseline Ca-Mg-Zn, Ca-Mg-Cu and Ca-Mg-Zn-Cu amorphous alloys. Thermal properties of these new metallic glasses, such as the glass transition, crystallization and melting temperatures, as well as heats of crystallization and melting, were determined and the effect of Al on GFA and GS of these alloys was identified.

2. Experimental Procedures

The alloys were prepared by induction melting mixtures of pure elements (in atomic percent, 99.99% for Al and Cu, 99.9% for Mg and Zn, and 99.5% for Ca) in a water-cooled copper crucible in an argon atmosphere. Each of the produced alloys was then induction re-melted in a quartz crucible with a 17.0 mm inner diameter and a ~2 mm diameter hole in the bottom of the crucible and cast through this hole into a water-cooled copper wedge-shaped mold to produce samples with thickness varying from 0.5 mm at the tip to 10 mm at the top. The amorphous or crystalline structure of the cast alloys was identified by X-ray diffraction of powdered samples using a Rigaku Rotaflex diffractometer, Cu K_{α} radiation, and by a differential scanning calorimeter (DSC) Q1000, by TA Instruments, Inc. The glass transition, T_g , and crystallization, T_x , temperatures, the temperatures of start, T_m , and completion, T_l , of melting, and heats of crystallization, ΔH_x , of the cast alloys were determined using DSC scans at a heating rate of 40 K/min. The maximum thickness, t_{max} , at which an alloy remained fully amorphous after water-cooled copper mold casting, was determined using X-ray diffraction and DSC patterns of samples extracted from several different-thickness regions of the wedge specimens. t_{max} was determined as the thickness above which the integral heat of crystallization, ΔH_x begins to

decrease from its maximum value with increasing sample thickness, and where sharp peaks from crystalline phases appear on the X-ray diffraction patterns. This method was validated and described in detail elsewhere [8]. The weight of samples used for DSC was in the range of 6 to 15 mg.

3. Results and Discussion

3.1. Ca-Mg-Al-Zn Metallic Glasses

The compositions of Ca-Mg-Al-Zn bulk metallic glasses produced in this work are shown in Table 1. Four Ca-Mg-Zn base alloys with different GFAs were used to study the effect of Al addition. These are Ca₅₅Mg₁₈Zn₂₇ (alloy #1, $t_{\max}=0.5$ mm), Ca₅₅Mg₂₀Zn₂₅ (alloy #4, $t_{\max}=2.0$ mm), Ca₆₀Mg₂₀Zn₂₀ (alloy #8, $t_{\max}=4.0$ mm), and Ca₆₀Mg₁₅Zn₂₅ (alloy #10, $t_{\max}=6.0$ mm). Substitution of Zn by 20at.% Al in alloy #1 increased t_{\max} to 1.0 mm (alloy #2); while substitution of the same amount of Zn with 5% Ca and 15% Al increased t_{\max} to 2.5 mm (alloy #3). When Al was added to alloy #4 (Ca₅₅Mg₂₀Zn₂₅), t_{\max} increased to 3.5 mm at 10% Al (alloy #5) and then decreased to 1.5 mm when the amount of Al further increased to 19% (alloys # 6 and 7). Addition of 10%Al to the Ca₆₀Mg₂₀Zn₂₀ alloy increased t_{\max} from 4.0 mm to 6.0 mm; but the same addition of Al to the alloy Ca₆₀Mg₁₅Zn₂₅ decreased t_{\max} from 6.0 mm to 4.0 mm (see alloys No. 8 to 11 in Table 1). One may conclude from these results that the GFA (i.e. t_{\max}) in the Ca-Mg-Zn alloys increases, approaches a maximum value and then decreases with an increasing substitution of Zn by Al.

Table 1 also shows that both T_g and T_x increase with partial substitution of Zn by Al. For example, in the Ca₅₅Mg₂₀Al_XZn_{25-X} series of alloys, T_g increases from 110°C to 175°C and T_x increases from 155°C to 211°C with an increase in Al from X = 0% to 19%. Figure 1 illustrates the effect of partial substitution of Zn by Al on crystallization and melting reactions in Ca-Mg-Al-Zn metallic glasses during continuous heating from an amorphous state. Not only T_g and T_x increase, but T_m and T_l also increase, the supercooled liquid, ΔT_x , and melting, ΔT_m , ranges become wider, heats of crystallization, ΔH_x , and melting, ΔH_m , increase, and crystallization occurs in a wider temperature range when the Al is added. ΔT_x increases from 30-48°C for alloys without Al to 36-71°C for the alloys with Al; however, no clear correlation between ΔT_x or t_{\max} was found for these alloys. A considerable increase in ΔT_m , from 41-83°C for the alloys without

Al to 80-197°C for the alloys with Al, indicates that the Al-containing alloys are far from eutectic compositions. A considerable increase in both T_g and T_x and broadening of the temperature interval for crystallization with the Al addition indicate that Al stabilizes the glassy state and slows crystallization in the Ca-Mg-Al-Zn system. The latter statement is also supported by the fact that the GFA may increase in spite of broadening of the melting (solidification) range with Al addition (see Table 1).

Typical X-ray diffraction patterns of a Ca-Mg-Al-Zn alloys versus the alloy thickness are shown in Figure 2. The patterns for $\text{Ca}_{60}\text{Mg}_{15}\text{Al}_{10}\text{Zn}_{15}$ illustrate transition from a fully amorphous to a partially crystalline state with an increase in alloy thickness from 4 mm to 10 mm. The critical cast thickness, t_{\max} , below which this alloy remains fully amorphous is 4 mm and when the thickness increases above t_{\max} , the alloy becomes partially crystalline. However, the presence of the crystal phases does not trigger further rapid crystallization, and even at the maximum produced thickness of 10 mm the alloy contains only ~20% of the amorphous phase. Such behavior of the Ca-Mg-Al-Zn alloys is quite different from the behavior of other Ca-based metallic glasses, which become fully crystalline in a much narrower thickness range after exceeding t_{\max} [4,8]. Evidently, aluminum stabilizes the glassy state in Ca-Mg-Al-Zn alloys and leads to formation of a composite structure consisting of the amorphous matrix and fine crystalline phases.

Figure 3 shows the density of $\text{Ca}_{55}\text{Mg}_{20}\text{Al}_x\text{Zn}_{25-x}$ metallic glasses as a function of the Al concentration. The density decreases linearly with an increase in the amount of Al from 2.24 g/cm³ for the alloy without Al to 1.85 g/cm³ for the alloy with 19% Al. The alloy $\text{Ca}_{60}\text{Mg}_{18}\text{Al}_{15}\text{Zn}_7$ has the lowest density of 1.84 g/cm³. Table 1 shows that there is no clear effect of Al addition on the reduced glass transition temperature ($T_{rg} = T_g/T_l$) and there is no correlation between t_{\max} and T_{rg} for these alloys.

3.2. Ca-Mg-Al-Cu Metallic Glasses

The compositions of Ca-Mg-Al-Cu bulk metallic glasses produced in this work are shown in Table 2. Four Ca-Mg-Cu base alloys with different GFAs were used to study the effect of Al addition. These are $\text{Ca}_{50}\text{Mg}_{20}\text{Cu}_{30}$ (alloy #12, $t_{\max}=8.0$ mm), $\text{Ca}_{50}\text{Mg}_{22.5}\text{Cu}_{27.5}$ (alloy #14, $t_{\max}=10.0$ mm), $\text{Ca}_{60}\text{Mg}_{20}\text{Cu}_{20}$ (alloy #16, $t_{\max}=4.0$ mm), and $\text{Ca}_{60}\text{Mg}_{15}\text{Cu}_{25}$ (alloy #19, $t_{\max}=1.0$ mm). In this alloy system, partial replacement of Cu by Al led to a considerable decrease in

GFA, with one exception. For example, addition of 10 at.% Al to $\text{Ca}_{50}\text{Mg}_{20}\text{Cu}_{30}$ decreased the critical thickness from 8 mm to 1 mm and addition of only 5 at.% Al to $\text{Ca}_{50}\text{Mg}_{22.5}\text{Cu}_{27.5}$ reduced t_{\max} from 10 mm to 3.5 mm. However, substitution of Cu by Al in alloy #19, which is a marginal glass former, led to an increase in GFA (compare alloys No. 19 and 20).

Figure 4 illustrates the effect of partial substitution of Cu by Al on crystallization and melting reactions in the Ca-Mg-Al-Cu metallic glasses during continuous heating from an amorphous state. Partial substitution of Cu by Al increases T_g and T_x ; however, the effect is not as strong as in the Ca-Mg-Zn alloys (compare Tables 1 and 2). The maximum values of T_g (143°C) and T_x (183°C) are observed in alloy $\text{Ca}_{50}\text{Mg}_{22.5}\text{Al}_5\text{Cu}_{22.5}$, which has a $t_{\max} = 3.5$ mm. This can be compared to $T_g = 158^\circ\text{C}$ and $T_x = 212^\circ\text{C}$ for the alloy $\text{Ca}_{60}\text{Mg}_{18}\text{Al}_{15}\text{Zn}_7$. Partial replacement of Cu by Al also increases ΔT_m and decreases T_{rg} . No systematic effect of Al addition was found on ΔH_x , ΔH_m and ΔT_x in the Ca-Mg-Al-Cu system. The density of these amorphous alloys decreases with an increase in the Ca, Mg and Al contents and a decrease in Cu. $\text{Ca}_{50}\text{Mg}_{20}\text{Cu}_{30}$ has the highest density of 2.46 g/cm³ and $\text{Ca}_{60}\text{Mg}_{20}\text{Al}_{10}\text{Cu}_{10}$ has the lowest density of 1.90 g/cm³ in this family of alloys.

3.3. Ca-Mg-Al-Zn-Cu Metallic Glasses

The composition of quaternary metallic glasses produced in this work is given in Table 3 and typical DSC patterns are shown in Figure 5. Two very good glass forming alloys, $\text{Ca}_{55}\text{Mg}_{18}\text{Zn}_{11}\text{Cu}_{16}$ and $\text{Ca}_{55}\text{Mg}_{18}\text{Zn}_{16}\text{Cu}_{11}$ which have a maximum amorphous thickness $t_{\max} > 10$ mm [10] were used as starting points; and from 5 to 15 % Al, as well as up to 5% Ca, were added to these alloys to reduce the density by partially replacing Cu and Zn. $\text{Ca}_{55}\text{Mg}_{18}\text{Zn}_{11}\text{Cu}_{16}$ and $\text{Ca}_{55}\text{Mg}_{18}\text{Zn}_{16}\text{Cu}_{11}$ have T_g of 102°C and 112°C and T_x of 166°C and 164°C, respectively, and densities of 2.32 and 2.31 g/cm³. Substitution of every 1 at% of Cu and/or Zn with Al and Ca decreases the density of these alloys by ~1% and 1.5%, respectively. For example, the densities of $\text{Ca}_{55}\text{Mg}_{18}\text{Al}_{15}\text{Zn}_6\text{Cu}_6$ and $\text{Ca}_{60}\text{Mg}_{18}\text{Al}_{15}\text{Zn}_3\text{Cu}_4$ alloys are 1.99 g/cm³ and 1.84 g/cm³, respectively (see Table 3). However, GFA reduces with Al addition. For example, partial replacement of Cu with 5 at% Al in $\text{Ca}_{55}\text{Mg}_{18}\text{Zn}_{11}\text{Cu}_{16}$ decreases the t_{\max} from >10mm to 9 mm. A further increase in Al to 10 and 15 at% decreases t_{\max} to 3 mm and 2.5 mm, respectively, in $\text{Ca}_{55}\text{Mg}_{18}\text{Al}_{10}\text{Zn}_{11}\text{Cu}_6$ and $\text{Ca}_{55}\text{Mg}_{18}\text{Al}_{15}\text{Zn}_6\text{Cu}_6$ alloys. At the same time, substitution of 5 at% Al with Ca in the alloy #27 leads to a $\text{Ca}_{60}\text{Mg}_{18}\text{Al}_{10}\text{Zn}_6\text{Cu}_6$ alloy with doubled the glass forming

ability ($t_{\max} = 5$ mm) and lower density of 1.94 g/cm^3 (see Table 3). X-ray diffraction patterns of this alloy at different thicknesses are shown in Figure 6. Only a diffuse amorphous halo is present at t up to 5mm; however, a number of peaks from crystalline phases are present on the X-ray diffraction pattern from a 7-mm thick region. Although it reduces the glass forming ability, addition of Al considerably improves the glass stability by increasing T_g and T_x (see Table 3 and Figure 5). For example, in the alloy $\text{Ca}_{55}\text{Mg}_{18}\text{Al}_{15}\text{Zn}_6\text{Cu}_6$ T_g and T_x are about 36°C and 11°C higher than in $\text{Ca}_{55}\text{Mg}_{18}\text{Zn}_{11}\text{Cu}_{16}$. The temperature range of super-cooled liquid has a tendency to slightly decrease with an increase in Al and it is in the range of $\Delta T_x = 41\text{--}56^\circ\text{C}$.

Addition of Al changes the crystallization and melting patterns of the $\text{Ca}_{55}\text{Mg}_{18}\text{Zn}_{11}\text{Cu}_{16}$ glassy alloy (see Figure 5). Crystallization of the amorphous alloy without Al starts at $\sim 166^\circ\text{C}$ and produces a sharp exothermic peak with a maximum at $\sim 171^\circ\text{C}$, which is followed by a smaller exothermic peak at $\sim 210^\circ\text{C}$. Melting of this alloy occurs in a rather narrow temperature range by a single endothermic reaction, indicating that the alloy may have a near eutectic composition. When 5% Cu is replaced by Al ($\text{Ca}_{55}\text{Mg}_{18}\text{Al}_5\text{Zn}_{11}\text{Cu}_{11}$), both crystallization peaks become wider and their maxima occur at higher temperatures, 184°C and 235°C , respectively. Such behavior indicates that Al reduces the crystallization kinetics. Melting also occurs at higher temperatures and is accompanied by multiple endothermic reactions within a much broader melting range (by about a factor of 2).

The first crystallization reaction is suppressed to a larger extent with further addition of Al up to 10 and 15 at% in place of Cu and Zn ($\text{Ca}_{55}\text{Mg}_{18}\text{Al}_{10}\text{Zn}_{11}\text{Cu}_6$ and $\text{Ca}_{55}\text{Mg}_{18}\text{Al}_{15}\text{Zn}_6\text{Cu}_6$), while the intensity of the second crystallization reaction almost does not change (see Figure 5). In addition, a third crystallization reaction occurs in these two alloys just prior to melting, and the T_m increases with an increase in Al content. The first melting reaction in the alloys with 10 and 15% Al starts rather slowly; the reaction rate gradually increases to a maximum value and then abruptly decreases to almost zero. After that, a weak and shallow melting reaction is observed in a wide temperature range, probably due to gradual melting of a primary phase.

Crystallization becomes even more complex in the $\text{Ca}_{60}\text{Mg}_{18}\text{Al}_{15}\text{Zn}_3\text{Cu}_4$ glass, and at least 5 crystallization exothermic peaks are recognized on a DSC pattern of this alloy. The melting range in the quintenary glasses is very wide, between 112°C for $\text{Ca}_{60}\text{Mg}_{18}\text{Al}_{15}\text{Zn}_3\text{Cu}_4$ and 221°C for $\text{Ca}_{55}\text{Mg}_{18}\text{Al}_{15}\text{Zn}_6\text{Cu}_6$. This provides an opportunity to design even better glass forming alloys

in this system by modifying the composition and reducing the temperature interval for melting (solidification).

It is well established for many glass forming systems, including Ca-Mg-Zn [8,16] and Ca-Mg-Cu [16], that the best glass forming alloys have a near-eutectic composition and slow crystallization kinetics [11,18]. The fact that the majority of the developed Ca-Mg-Al-Zn, Ca-Mg-Al-Cu and Ca-Mg-Al-Zn-Cu glassy alloys have a very wide melting range indicate that their compositions are far from the eutectic composition, and even better glass forming ability and larger maximum amorphous thicknesses are expected in optimized alloy compositions with a considerably reduced melting range.

3.4. Effect of Al on Structure of the Ca-Mg-Zn-Cu Glasses

A recently developed efficient cluster packing (ECP) model [19,20] was used to analyze likely structural changes of Ca-Mg-Zn-Cu metallic glasses by additions of Al. In this model, a structural scaffold is comprised of interpenetrating solute-centered clusters formed with the largest solute, α , and in which solvent atoms (Ω) dominate the 1st coordination shell. The α clusters are organized at positions that approximate those of an fcc structure over a limited length scale of several cluster diameters, beyond which recognizable order of the cluster positions is probably lost. This structure has two additional progressively smaller sites; β sites occur at the center of an octahedron of α -centered clusters, and γ sites are at the center of a tetrahedron of α clusters. There are 1 β and 2 γ sites for every α site. It is assumed that α sites are filled by α solutes, but β and γ sites can be progressively filled by any solute. A small number of solutes may also occupy Ω sites. A nomenclature describes the structure by the local coordination numbers of α , β and γ solutes, $\langle N_{\alpha}, N_{\beta}, N_{\gamma} \rangle$, as determined from the relative solute sizes. The chemical descriptions for metallic glasses used here give the solvent species first, followed by solutes in order of decreasing size. Solutes with nearly equivalent sizes are listed in parentheses to indicate that they are topologically identical and are likely to occupy the same structural sites. Alloy compositions are listed in atomic percent following each atomic species in the alloy. Additional details of the ECP model and justification for these basic assumptions are given elsewhere, along with an assessed table of atomic radii for metallic glass structures [20].

The putative number of Ca atoms that can efficiently pack around a Mg atom is ~10, and around a Zn atom is ~9, so that Ca-Mg-Zn ternary glasses have $\langle 10,9 \rangle$ structures. The α sites are filled by Mg and the β and γ sites are filled by combinations of Mg and Zn. Since the radius ratios of Al and Zn relative to the radius of Ca are within about 2% of each other (0.726 and 0.701, respectively), substitution of Zn by Al should not change the glass structure, and Ca-Mg-Al-Zn glasses retain a $\langle 10,9 \rangle$ topological structure. The α sites are filled by Mg and the β and γ sites are filled by combinations of Mg, Al and Zn. Although the topological structure remains unchanged, GFA and GS both improve when Zn is partially substituted by Al, which evidently indicate that the amorphous structure becomes more stable. The addition of small amounts of Al, which atoms are slightly larger than those of Zn, may provide more flexibility for denser atomic packing, reducing internal stresses, and, therefore, reducing the free energy. Alternatively, the Al additions may provide a favorable chemical contribution to stability of these glasses.

Ca-Mg-Cu alloys are topological ternary glasses with a $\langle 10,8 \rangle$ structural designation, indicating that only 8 Ca atoms can efficiently pack around a Cu atom. Partial substitution of Cu with Al transforms these glasses into topologically quaternary glasses $\langle 10,9,8 \rangle$. A composition of $\text{Ca}_{61}\text{Mg}_{13}\text{Al}_{13}\text{Cu}_{13}$ is estimated when the α and β sites are filled by Mg and Al, respectively, and the γ sites are half-filled with Cu. The three solute-lean glasses studied here in this family of alloys (Table 2) fit this model closely, with some small fraction of the solutes occupying solute sites other than the preferred or ‘native’ sites. When all of the γ sites are filled by Cu, the ECP model gives a composition of $\text{Ca}_{54}\text{Mg}_{11.5}\text{Al}_{11.5}\text{Cu}_{23}$. The two solute-rich glasses in this family are close to this composition, again with some substitutions amongst the solute sites and a small number of Ω sites occupied by solutes in excess of those that can be accommodated on α , β and γ sites. Ca and Cu have strong covalent bonding [10] and large negative heats of mixing [11], which probably contribute to the very good GFA of ternary Ca-Mg-Cu alloys. Partial substitution of Cu by Al weakens the average bond strength, and, therefore, reduces GFA. A slight improvement of the glass stability of these alloys against crystallization with the Al addition can be explained by more complex structure of the quaternary alloys, which restricts atomic rearrangements.

Ca-Mg-(Al,Zn)-Cu are $\langle 10,9,8 \rangle$ topological quaternary glasses, where Mg occupies α positions, Al and Zn occupy β positions and Cu occupies γ positions as preferred sites. In the three

compositions where the Ca concentration is 55% (Table 3), the α , β and γ sites are filled by solutes. A fraction of the β or γ sites are not occupied by solutes in glasses where the Ca concentration is 60%. In accord with the above discussion, partial substitution of Zn by Al may improve both GFA and GS, while partial substitution of Cu by Al in this alloy system should reduce GFA and may slightly improve GS. Although a large number of different alloys are not presently available to support these statements, there is however evidence that Al indeed improves glass stability in this system; while GFA reduces not as dramatically as in the Ca-Mg-Cu system (for example, compare alloys 14, 15, and 21, 23).

5. Conclusions

The effect of Al additions on the glass forming ability (GFA, given as the maximum fully amorphous thickness, t_{max}) and stability against crystallization (measured by the glass transition, T_g , and crystallization, T_x , temperatures) of Ca-Mg-Zn, Ca-Mg-Cu and Ca-Mg-Zn-Cu alloys was studied. Ca-Mg-Zn, Ca-Mg-Cu and Ca-Mg-Zn-Cu have very good GFA; however, the stability of these glasses is low (low T_g and T_x). The addition of Al improves glass stability in these alloys by increasing T_g and T_x and slowing the crystallization kinetics. However, the temperature range of melting ($\Delta T_m = T_l - T_m$) increases considerably, which indicates that the Al additions move the alloys far from the eutectic compositions. In the Cu-containing alloys this increase in ΔT_m generally results in a decrease in t_{max} . However, in the Ca-Mg-Zn and some Ca-Mg-Cu based alloys t_{max} increases with Al addition, regardless of an increase in ΔT_m . It is therefore expected that even better glass formers can be found in these alloy systems by modifying the compositions and reducing the ΔT_m range. Each 1 at.% Al substituting Cu and/or Zn reduces the alloy density by about 1% and several bulk metallic glasses produced in this work have densities below 1.9 g/cm³.

The compositions of these alloys provide efficiently packed cluster structures. Application of the efficient cluster packing model suggests that these glasses are formed by efficiently-packed Mg-centered clusters where Al and Zn are preferred at cluster-octahedral β sites, and Cu is native to cluster-tetrahedral γ sites. A significant amount of interchangeability between Al, Zn and Cu solutes seems to be supported in this family of glasses. Ca-Mg-(Al,Zn) are represented as <10,9>

topological ternary glasses, while Ca-Mg-Al-Cu and Ca-Mg-(Al,Zn)-Cu are <10,9,8> topological quaternary glasses.

6. Acknowledgements

This work was conducted at the Air Force Research Laboratory, Materials and Manufacturing Directorate, under an on-site contract No. FA8650-04-D-5233. Funding through AFOSR Task 01ML05-COR (Capt. B. Connor, Program Manager) is greatly appreciated.

References

1. K. Amiya and A. Inoue: Mater. Trans. JIM **43** (2002) 81-84.
2. K. Amiya and A. Inoue: Mater. Trans. JIM **43** (2002) 2578-2581.
3. O.N. Senkov and J.M. Scott: *MRS Proceedings*, Vol. 806, (Materials Research Society, Warrendale, PA, 2003) pp.145-150.
4. O.N. Senkov and J.M. Scott: Mater. Letters **58** (2004) 1375-1378.
5. O.N. Senkov and J.M. Scott: Scripta Materialia **50** (2004) 449-452.
6. E.S. Park and D.H. Kim: J. Mater. Research **19** (2004) 685-688.
7. F.Q. Guo, S.J. Poon and G.J. Shiflet: Appl. Phys Letters **84** (2004) 37-39.
8. O.N. Senkov and J.M. Scott: J. Non-Cryst. Solids **351** (2005) 3087-3094.
9. E.S. Park, W.T. Kim and D.H. Kim: Mater. Sci. Forum **475-479** (2005) 3415-3418.
10. O.N. Senkov, D.B. Miracle and J.M. Scott: Intermetallics **14** (2006) 1055-1060.
11. A. Takeuchi, A. Inoue, Mater. Trans. JIM **46** (2005) 2817-2829.
12. Z. Zhang, V. Keppens, O.N. Senkov and D.B. Miracle: Mater. Sci. Eng. A (2007).
13. M.L. Morrison, R.A. Buchanan, O.N. Senkov, D.B. Miracle and P.K. Liaw: Metall. Mater. Trans. A **37A** (2006) 1239-1245.
14. B. R. Barnard, P. K. Liaw, R. A. Buchanan, O. N. Senkov and D. B. Miracle: Mater. Trans. JIM (2007, in press).
15. J.E. Dahlman, O.N. Senkov, J.M. Scott and D.B. Miracle: Mater. Trans. JIM (2007, in press).
16. S. Gorsse, G. Orveillon, O.N. Senkov and D.B. Miracle: Physical Review B **73** (2006) 224202-1-9.
17. O.N. Senkov, J.M. Scott, and D.B. Miracle: J. Alloys Compounds **424** (2006) 394-399.
18. A Inoue, Acta Metarialia **48** (2000) 279-306.
19. D.B. Miracle: Nature Materials **3** (2004) 697-702.
20. D.B. Miracle: Acta Materialia **54** (2006) 4317-4336.

TABLES

Table 1. Compositions (in at%) of Ca-Mg-Al-Zn amorphous alloys and their critical thickness, t_{\max} , glass transition, T_g , and crystallization, T_x , temperatures, the temperatures of start, T_m , and completion, T_l , of melting, heats of crystallization, ΔH_x , and melting, ΔH_m , the temperature intervals of melting, $\Delta T_m = T_l - T_m$, and supercooled liquid, $\Delta T_m = T_x - T_g$, reduced glass transition temperature $T_{rg} = T_g/T_l$ and the alloy density.

No.	Composition (at.%)	t_{\max} (mm)	T_g (°C)	T_x (°C)	T_m (°C)	T_l (°C)	ΔH_x (J/g)	ΔH_m (J/g)	ΔT_m (°C)	ΔT_x (°C)	T_g/T_l (K/K)	ρ (g/cm ³)
1	Ca ₅₅ Mg ₁₈ Zn ₂₇	0.5	116	146	350	398	70	115	48	30	0.580	2.29
2	Ca ₅₅ Mg ₁₈ Al ₂₀ Zn ₇	1.0	174	218	352	549	76	189	197	44	0.544	1.88
3	Ca ₆₀ Mg ₁₈ Al ₁₅ Zn ₇	2.5	158	212	348	475	110	203	127	54	0.576	1.84
4	Ca ₅₅ Mg ₂₀ Zn ₂₅	2.0	110	155	346	429	82	170	83	45	0.546	2.24
5	Ca ₅₅ Mg ₂₀ Al ₁₀ Zn ₁₅	3.5	130	196	358	500	86	179	142	66	0.521	2.03
6	Ca ₅₅ Mg ₂₀ Al ₁₅ Zn ₁₀	2.0	148	204	354	533	91	262	179	56	0.522	1.93
7	Ca ₅₅ Mg ₂₀ Al ₁₉ Zn ₆	1.5	175	211	358	472	92	223	114	36	0.601	1.85
8	Ca ₆₀ Mg ₂₀ Zn ₂₀	4.0	105	142	336	387	90	153	51	37	0.573	2.08
9	Ca ₆₀ Mg ₂₀ Al ₁₀ Zn ₁₀	6.0	130	176	354	473	95	181	119	46	0.540	1.89
10	Ca ₆₀ Mg ₁₅ Zn ₂₅	6.0	106	154	336	377	92	143	41	48	0.583	2.21
11	Ca ₆₀ Mg ₁₅ Al ₁₀ Zn ₁₅	4.0	130	201	350	430	99	124	80	71	0.573	2.01

Table 2. Compositions (in at%) of Ca-Mg-Al-Cu amorphous alloys and their glass transition, T_g , and crystallization, T_x , temperatures, the temperatures of start, T_m , and completion, T_l , of melting, the temperature range of melting, $\Delta T_m = T_l - T_m$, the supercooled liquid range $\Delta T_m = T_x - T_g$, heats of crystallization, ΔH_x , and melting, ΔH_m , the maximum thickness, t_{\max} , reduced glass transition temperature, $T_{rg} = T_g/T_l$, and density, ρ .

No.	Composition (at.%)	t_{\max} (mm)	T_g (°C)	T_x (°C)	T_m (°C)	T_l (°C)	ΔH_x (J/g)	ΔH_m (J/g)	ΔT_m (°C)	ΔT_x (°C)	T_g/T_l (K/K)	ρ (g/cm ³)
12	Ca ₅₀ Mg ₂₀ Cu ₃₀	8.0	128	169	354	417	139	378	63	41	0.581	2.46
13	Ca ₅₀ Mg ₂₀ Al ₁₀ Cu ₂₀	1.0	138	168	384	458	96	227	74	30	0.562	2.22
14	Ca ₅₀ Mg _{22.5} Cu _{27.5}	10	127	169	354	390	150	208	36	42	0.603	2.39
15	Ca ₅₀ Mg _{22.5} Al ₅ Cu _{22.5}	3.5	143	183	354	489	100	188	135	40	0.546	2.27
16	Ca ₆₀ Mg ₂₀ Cu ₂₀	4.0	114	139	356	405	105	181	49	25	0.571	2.11
17	Ca ₆₀ Mg ₉ Al ₁₁ Cu ₂₀	2.0	128	177	383	482	117	185	99	49	0.530	2.17
18	Ca ₆₀ Mg ₂₀ Al ₁₀ Cu ₁₀	2.0	135	169	390	544	96	210	154	34	0.499	1.90
19	Ca ₆₀ Mg ₁₅ Cu ₂₅	1.0	123	155	354	414	99	205	60	32	0.576	2.25
20	Ca ₆₀ Mg ₁₅ Al ₁₀ Cu ₁₅	2.0	124	157	384	416	103	165	32	33	0.490	2.03

Table 3. Compositions (in at%) of Ca-Mg-Al-Zn-Cu amorphous alloys and their critical thickness, t_{\max} , glass transition, T_g , and crystallization, T_x , temperatures, the temperatures of start, T_m , and completion, T_l , of melting, heats of crystallization, ΔH_x , and melting, ΔH_m , the temperature intervals of melting, $\Delta T_m = T_l - T_m$, and supercooled liquid, $\Delta T_m = T_x - T_g$, reduced glass transition temperature $T_{rg} = T_g/T_l$ and the alloy density.

No.	Composition (at.%)	t_{\max} (mm)	T_g (°C)	T_x (°C)	T_m (°C)	T_l (°C)	ΔH_x (J/g)	ΔH_m (J/g)	ΔT_m (°C)	ΔT_x (°C)	T_g/T_l (K/K)	ρ (g/cm ³)
21	Ca ₅₅ Mg ₁₈ Zn ₁₁ Cu ₁₆	>10	102	166	330	363	95	162	33	66	0.586	2.32
22	Ca ₅₅ Mg ₁₈ Zn ₁₆ Cu ₁₁	>10	112	164	331	352	110	172	21	53	0.614	2.31
23	Ca ₅₅ Mg ₁₈ Al ₅ Zn ₁₁ Cu ₁₁	9	119	175	331	513	114	192	182	56	0.499	2.22
24	Ca ₅₅ Mg ₁₈ Al ₁₀ Zn ₁₁ Cu ₆	3	128	171	341	562	101	228	221	43	0.480	2.09
25	Ca ₅₅ Mg ₁₈ Al ₁₅ Zn ₆ Cu ₆	2.5	136	177	360	581	95	293	221	41	0.479	1.99
26	Ca ₅₅ Mg ₁₅ Al ₁₀ Zn ₁₅ Cu ₅	6	105	148	334	558	94	211	224	43	0.455	2.17
27	Ca ₆₀ Mg ₁₈ Al ₁₀ Zn ₆ Cu ₆	5	134	176	357	530	128	211	173	42	0.507	1.94
28	Ca ₆₀ Mg ₁₈ Al ₁₅ Zn ₃ Cu ₄	2	144	195	370	503	123	193	123	51	0.552	1.84

FIGURES

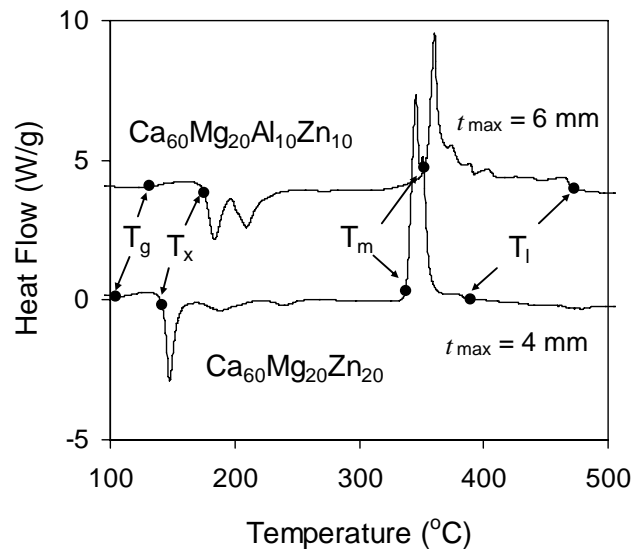


Figure 1. Effect of partial substitution of Zn by Al on glass transition, crystallization and melting reactions in $\text{Ca}_{60}\text{Mg}_{20}\text{Zn}_{20}$ and $\text{Ca}_{60}\text{Mg}_{20}\text{Al}_{10}\text{Zn}_{10}$ metallic glasses during continuous heating with the heating rate of $40^{\circ}\text{C}/\text{min}$. Endothermic reactions are directed up. Characteristic temperatures are indicated by arrows, and the alloy compositions and their critical amorphous thicknesses are shown near the corresponding curves.

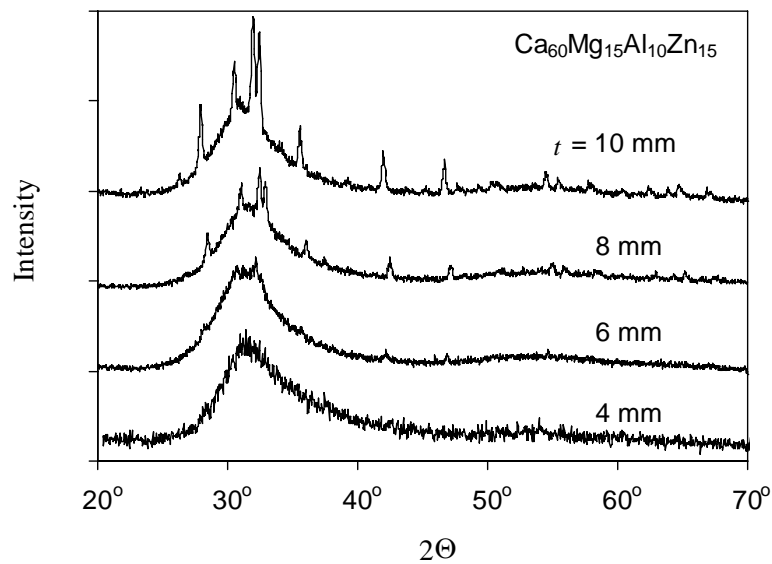


Figure 2. X-ray diffraction patterns of cast $\text{Ca}_{60}\text{Mg}_{15}\text{Al}_{10}\text{Zn}_{15}$ samples of different thicknesses (shown near the corresponding curves).

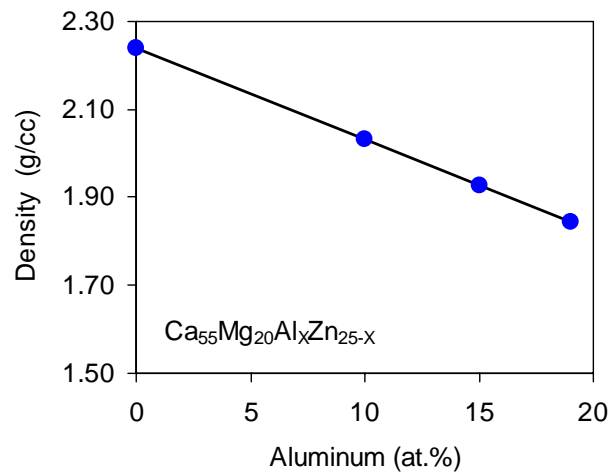


Figure 3. Density of $\text{Ca}_{55}\text{Mg}_{20}\text{Al}_X\text{Zn}_{25-X}$ metallic glasses versus the concentration of Al (X).

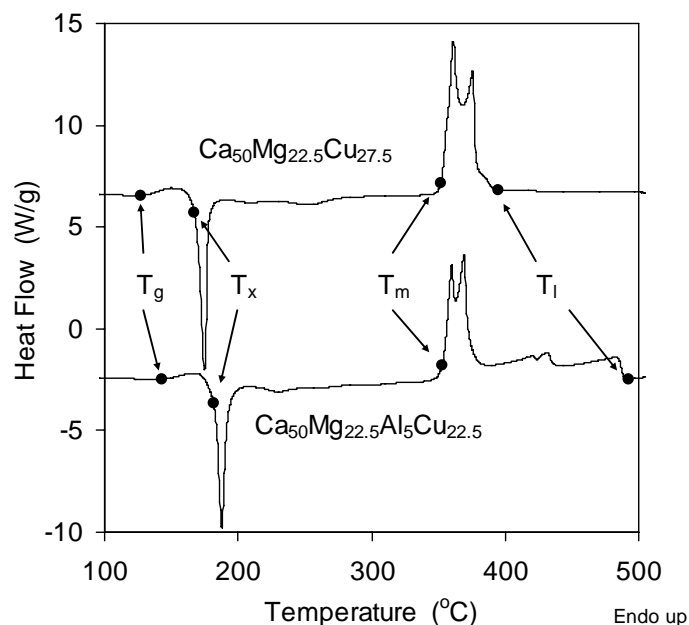


Figure 4. Effect of partial substitution of Cu by Al on glass transition, crystallization and melting reactions in $\text{Ca}_{50}\text{Mg}_{22.5}\text{Cu}_{27.5}$ and $\text{Ca}_{50}\text{Mg}_{22.5}\text{Al}_5\text{Cu}_{22.5}$ metallic glasses during continuous heating with the heating rate of $40^\circ\text{C}/\text{min}$. Endothermic reactions are directed up. Characteristic temperatures are indicated by arrows, and the alloy compositions and their critical amorphous thicknesses are shown near the corresponding curves.

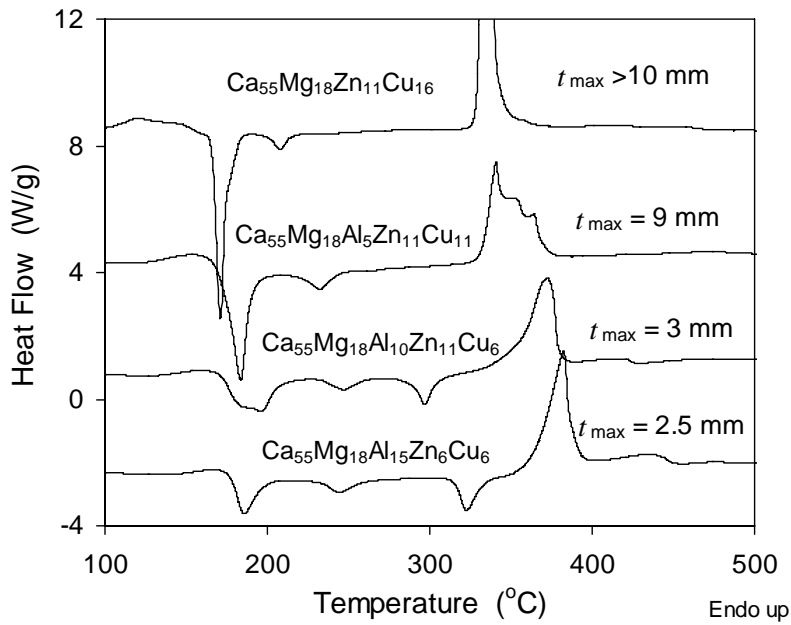


Figure 5. DSC heating curves of $\text{Ca}_{55}\text{Mg}_{18}\text{Al}_{x+Y}\text{Zn}_x\text{Cu}_Y$ metallic glasses showing the effect of Al additions on glass transition, crystallization and melting reactions.

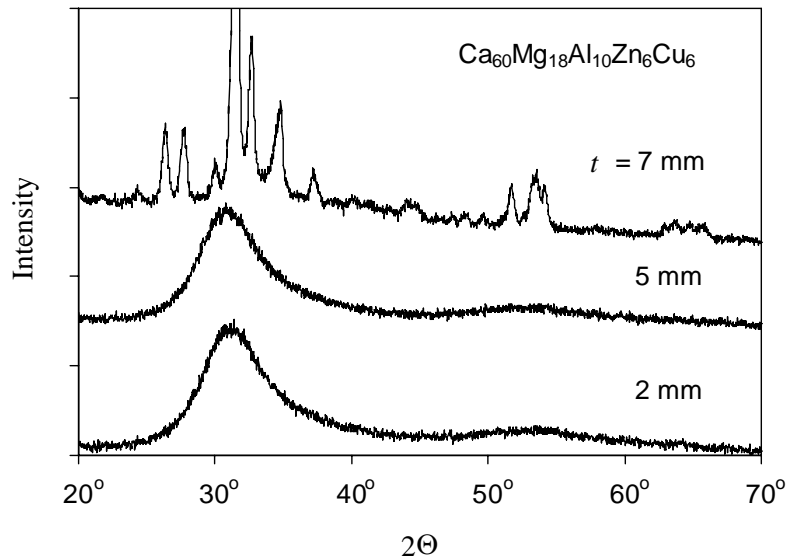


Figure 6. X-ray diffraction patterns of cast $\text{Ca}_{60}\text{Mg}_{18}\text{Al}_{10}\text{Zn}_6\text{Cu}_6$ samples of different thicknesses (shown near the corresponding curves).